



---

Laval (Greater Montreal)

June 12 - 15, 2019

## **BEHAVIOUR OF 27-YEAR OLD PRESTRESSED CONCRETE BRIDGE GIRDERS**

Zhaohan Wu<sup>1,2</sup>, Douglas Tomlinson<sup>1</sup>, and Carlos Cruz-Noguez<sup>1</sup>.

<sup>1</sup> University of Alberta, Canada

<sup>2</sup> zhaohan@ualberta.ca

**Abstract:** Recently a bridge on Highway 763 in Alberta, built in 1991, was closed due to serious deterioration. During subsequent inspections, it was found that the material properties of these bridge girders are unclear. There are several bridges in Alberta that have the similar structural design, so the scope of this project is to investigate the damage and give a good understanding of why this bridge's girders deteriorated so quickly. The first stage of this project is to use the original properties of the damaged girder to calculate moment capacity of the "as new girder". VecTor2 is used to calculate the moment capacity of the original girders. This finite element modeling program can give reaction forces as an output with a corresponding failure mode. Later on, experimental testing will be carried out on these 9 damaged girders to assess the failure modes. Each girder tested using a flexure cracking test to determine the actual capacity. All girders are simply supported on 4 steel pedestals with electrometric bearing pads. In order to achieve 4-point bending, a spreader beam is placed on top of the experimental girder to distribute the forces from hydraulic actuator. The experimental result will be compared with the modeling data to see how the deterioration affected the capacity of these girders. The finite element modelling method showed a capacity of 1358 KNm for the "as new girder". The girder fails in flexure and concrete crushed after steel yields. This capacity data provided by VecTor2 gives a good understanding of how these girders will perform under testing.

### **1 INTRODUCTION**

Prestressed concrete is one of the favoured construction materials for bridges in Alberta due to its improved stiffness and cost-savings compared to normal reinforced concrete. Since the 1970s, hundreds of prestressed concrete bridges were built around Alberta. However, highway bridges are prone to chemical attacks from chlorides, sulfates, or alkali-silica reaction (Enright and Frangopol 1998). These chemical attacks will eventually lead to steel corrosion, which significantly affects the strength of the bridge. It is important to understand and predict the service life of deteriorated bridges, because maintenance, rehabilitation, and replacement costs are very expensive. The behaviour of deteriorated bridges is hard to predict, because of inconsistency of the designs compared to those originally designed using the Canadian Highway Bridge Design Code (CISC 2014). The bridge code is relatively conservative for pristine bridges, but as bridges deteriorate the code strength predictions will become progressively less conservative, which may lead to failure of the bridge in service.

In this paper, a case study bridge located on Highway 763 near Barrhead, Alberta (~150 km northwest of Edmonton) is examined. The bridge is a single span structure with a length of 11 m; is comprised of 510 mm deep prestressed hollow core box girders without a topping. This bridge was closed to traffic and then removed due to serious deteriorations discovered in an inspection in late 2017. As shown in Figure

1, the cover of the bridge had fallen off leaving steel reinforcement exposed, which led to serious corrosion. This bridge, built in 1991, is consisted of 9 girders where 7 are box girders and 2 are barrier girders. One of the issues of these bridge girders are the designs are unclear: the steel reinforcement design is vague and hard to identify; the actual density and strength of concrete of the girder is also unclear. Unfortunately, there are many bridges with a similar design in Alberta, it is important to figure out the cause for the deteriorations in order to know how to maintain and repair other bridges with similar damages. In this paper, a single interior box girder taken from is discussed.



Figure 1. The Deterioration of the Case Study Bridge

## 2 MODELING

### 2.1 Introduction of VecTor 2

The first stage of this project is to determine the original capacity of the box girder. The original properties of the bridge girder obtained from Alberta Transportation (2018) were used to build the model. VecTor 2 is used to construct this model. VecTor 2 is a non-linear finite element analysis program for two dimensional reinforced concrete structures. The material properties can be inputted before hand into the program, later on a corresponding failure mode will be provided after running the model. VecTor2 is based on the Modified Compression Field Theory (MCFT) formulated by Vecchio and Collins (1986), and the Disturbed Stress Field Model (DSFM) proposed by Vecchio (2000). In these formulations, the concrete is modeled as an orthotropic material with smeared, rotating cracks. Complete details on the MCFT and DSFM implementation in Vector2 can be found elsewhere (Wong and Vecchio, 2002).

### 2.2 Girder Properties

The box girder is 11m long, 1.2m wide and 510 mm in height. As shown in Figure 2, the girder contains three 300mm voids. The girder is prestressed with twenty 12 mm diameter 7-wire low-relaxation pretensioning strands with an ultimate strength of 1860 MPa. The girder also is reinforced with seven 10M mild steel bars with specified yield strength of 400MPa. The number and layout of the reinforcement from bottom to top are shown in Table 1. There are 4 layers of reinforcement in the box girder. The bottom layer has the most reinforcements (14 pretensioning bars and 2 mild steel bars). The remaining layers have two pretensioning strands each. The top layer has 5 additional 10M mild steel reinforcements.

Table 1. Number and Type of Reinforcement

| Layer        | Distance From bottom, mm | Number of 7-wire 12 mm diameter Pretensioning Strands | Number of 10M Mild Steel Bars |
|--------------|--------------------------|---|-------------------------------|
| First layer  | 60                       | 14  | 2                             |
| Second layer | 110                      | 2   | 0                             |
| Third layer  | 340                      | 2   | 0                             |
| Fourth layer | 440                      | 2   | 5                             |

The concrete in girder is made of structural lightweight concrete with a density of  $1920 \text{ kg/m}^3$ . The specified 28-day strength of the concrete is 35 MPa. These properties mentioned above were used as inputs in VecTor 2.

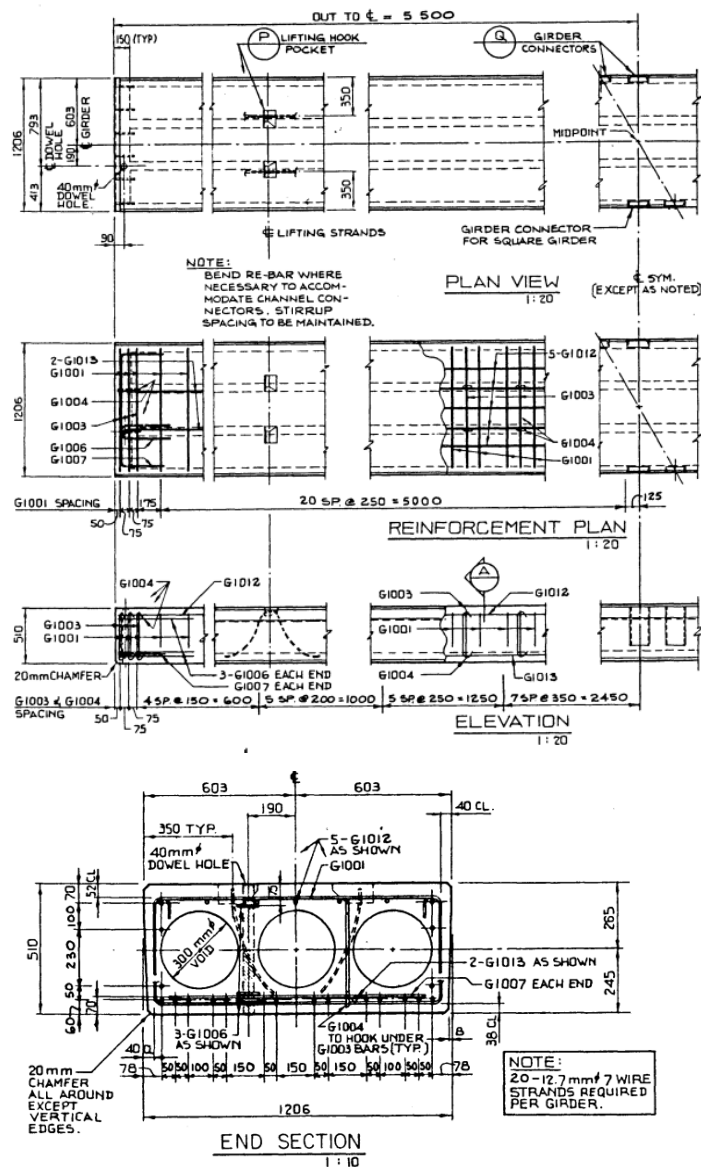


Figure 2. The Design Plan of the Box Girder (Alberta Transportation 2018)

### 2.3 Modelling of Concrete

The constitutive relationships used to model the concrete were selected from the library of models in VecTor2. For the post-peak response, the modified Park-Kent model was selected. This model was implemented in VecTor2 by Wong and Vecchio (2002) as follows:

$$f_{ci}^b = -\left[ f_p + Z_m f_p (\varepsilon_{ci} - \varepsilon_p) \right] < 0 \quad \text{or} \quad -0.2 f_p \quad \text{for} \quad \varepsilon_{ci} < \varepsilon_p < 0 \quad (1)$$

where

$$Z_m = \frac{0.5}{\frac{3 + 0.29 |f'_c|}{145 |f'_c| - 1000} \left( \frac{\varepsilon_0}{-0.002} \right) + \left( \frac{|f_{lat}|}{170} \right)^{0.9} + \varepsilon_p} \quad (f'_c \text{ and } f_{lat} \text{ in MPa}) \quad (2)$$

$\varepsilon_0$  is the concrete compressive strain associated to the cylinder compressive strength,  $f'_c$ , and  $f_{lat}$  is the summation of principal stresses acting transversely to the direction under consideration.

All properties were input into VecTor 2. As shown in Table 2 and 3, the properties of concrete and steel were input separately into the software. To account for the voids within the girder, the concrete materials are divided into 8 layers with 4 different thicknesses in the model; therefore, 4 different types of materials with different thicknesses are needed as shown in Table 2. The thickness of the concrete was calculated using the end view of the girder in Figure 2. The length of the void was subtracted when calculating the thickness of different layers. The known properties were inputted into the model such as density and strength of concrete. The rest of the unknown properties were set to default by the software. There are no smeared reinforcement components in the concrete; the shear reinforcement was modeled separately.

Table 2. Material Properties of Concrete

| Reinforced concrete | Thickness (mm) | Compressive strength (Mpa) | Density (kg/m <sup>3</sup> ) |
|---------------------|----------------|----------------------------|------------------------------|
| Material 1          | 1206           | 35                         | 1902                         |
| Material 2          | 606            | 35                         | 1902                         |
| Material 3          | 456            | 35                         | 1902                         |
| Material 4          | 336            | 35                         | 1902                         |

### 2.4 Modelling of Steel Rebar and Stirrups

Steel reinforcement properties were assigned for each concrete layer defined in section 2.3. The total cross sectional area and material properties were inputted in the model. Reinforcement was inputted as trusses within the concrete layers. There are 4 layers of steel reinforcement according to the end view of the girder in Figure 2; each layer of reinforcement was assigned into the corresponding concrete layer. Different reinforcement types were added separately into the concrete layer. As shown in Table 3, prestressing steel and mild reinforcement were added separately with different layer cross-sectional areas. The five types of reinforcements with different cross sectional area shown in Table 3 are: the prestressing steel at the bottom layer (total cross-sectional area of 1382mm<sup>2</sup>), mild reinforcement at the bottom layer with a total cross-sectional area of 200mm<sup>2</sup>, 3 sets of two prestressing steels with same total cross-sectional area of 197mm<sup>2</sup> in the middle and top layers, mild reinforcement with a cross-sectional area of 500mm<sup>2</sup> on the top layer, and mild steel shear reinforcement with a cross-sectional area of 100mm<sup>2</sup> (10M bars). The stress and strain response is the perfect elastic and then perfect plastic, which means no strain hardening after yielding. To model the stirrups, the stirrups were defined as trusses as shown in Figure 3 in green. The stirrup spacing was designed using the design plan in Figure 2. The

discrete modelling of stirrups were preferred over smeared stirrups in this modelling, because it better mimics the true nature of stirrups in the bridge girder than a smear reinforcement ratio. Inputting Smeared reinforcement ratio into concrete materials allows the model to input small shear reinforcements in all the concrete layers; this will likely give a higher shear strength than inputting the discrete stirrups.

Table 3. Material Properties of Steel Reinforcements

| Type                  | Cross Section Area (mm <sup>2</sup> ) | Diameter (mm) | Yield Strength (MPa) | Ultimate Strength (MPa) | Elastic Modulus (MPa) | Strain Hardening (me) | Ultimate Strain (me) | Prestrain (me) |
|-----------------------|---------------------------------------|---------------|----------------------|-------------------------|-----------------------|-----------------------|----------------------|----------------|
| Steel 1 Prestressing  | 1381.8                                | 12.7          | 1670                 | 1860                    | 200000                | 9                     | 30                   | 6.5            |
| Steel 2 Ductile steel | 200                                   | 10            | 400                  | 600                     | 200000                | 10                    | 150                  | 0              |
| Steel 3 Prestressing  | 197.4                                 | 12.7          | 1670                 | 1860                    | 200000                | 9                     | 30                   | 6.5            |
| Steel 4 Ductile steel | 500                                   | 10            | 400                  | 600                     | 200000                | 10                    | 150                  | 0              |
| Steel 5 Ductile steel | 100                                   | 10            | 400                  | 600                     | 200000                | 10                    | 150                  | 0              |

## 2.5 Geometric modeling

The finite element model of this study is shown below in Figure 3. The concrete layers and steel trusses mentioned in 2.3 and 2.4 were constructed using coordinates that correspond to those in the actual bridge design. The concrete was modelled using a rectangular mesh with the size of 40 x 40 mm. This modelled girder is simply supported with displacement controlled loading. The loading span and location of the supports were based on the planned experimental setup in elevation view from Figure 4.

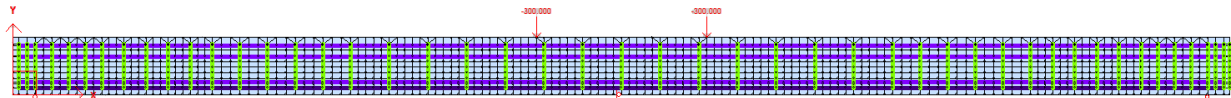


Figure 3. Finite Element Model of 11m Long Girder

## 3 EXPERIMENTAL PROGRAM

### 3.1 Test Setup

The 11m long girder will be tested under four-point bending test using an MTS6000 (capacity 6000 kN) loading frame and actuator. As shown in Figure 4, the girder is simply supported on steel pedestals. Hollow Structural Sections (HSS) are used as a transverse beam to distribute the width of the girder to the top of the supports. A neoprene pad is placed on top of the hollow sections to mimic the true bridge girder's support conditions. The HSS were welded and bolted on top of the support to keep them from slipping during testing. Four-point bending test is achieved using a spreader beam on top the girder to distribute the forces from the hydraulic actuator.

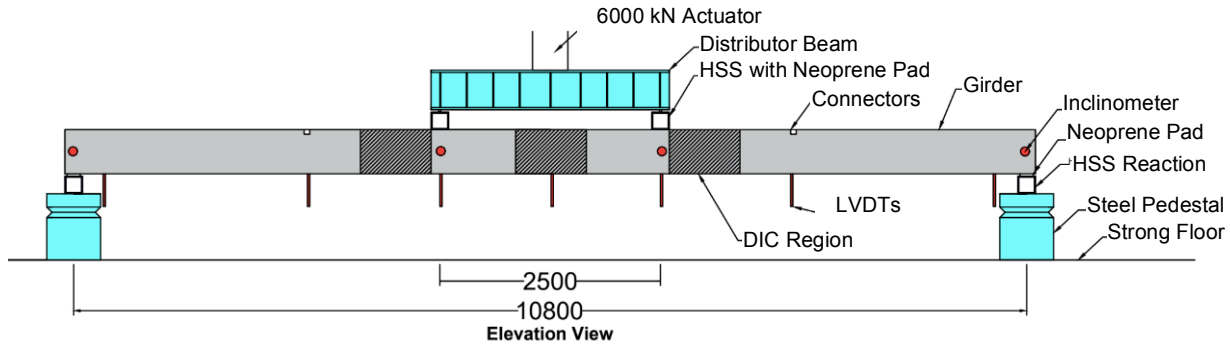


Figure 4. Designed Test Setup (dimensions in mm)

### 3.2 Instrumentations

Instrumentation system consists of Linear Variable Differential Transformers (LVDT) or string potentiometers for deflection measurements, inclinometers for rotation measurements, and Digital Image Correlation (DIC) for crack and deflection measurement at midspan and immediately within the shear span regions. LVDTs and string potentiometers will be used at five points along the span to track the deflected shape of the beam, particularly at the connector points between girders as this will allow for future assessments on load-sharing between girders. 25 mm LVDTs will be used at the location of neoprene pads to account for compression of the pads. Inclinometers measuring rotation will be placed at the supports and loading points. DIC is a method that compares digital photographs of a test piece at different stages of deformation. It can build up 2D and 3D vector field and strain maps by tracking blocks of pixels (McCormick and Lord 2010). DIC will be used to measure deflection and track the formation and widths of cracks in the girder. Three cameras will be used to focus separately on the shear spans and midspan of the girder.

## 4 RESULTS AND DISCUSSION

### 4.1 VecTor 2 Model

The results calculated with VecTor 2 are summarized in Figure 5. The expected additional (i.e. in addition to self-weight) load that the girder can handle is 500 kN at a midspan deflection of 113.4 mm. The camber calculated by VecTor 2 is around 18.2mm before loading. The magnified displacement and crack pattern figure from the model is shown in Figure 6; deep flexure and shear cracks can be seen in the loading region. This corresponding failure mode of the girder and the capacity curve indicate that the girder fails in flexure with concrete crushing after steel yields.

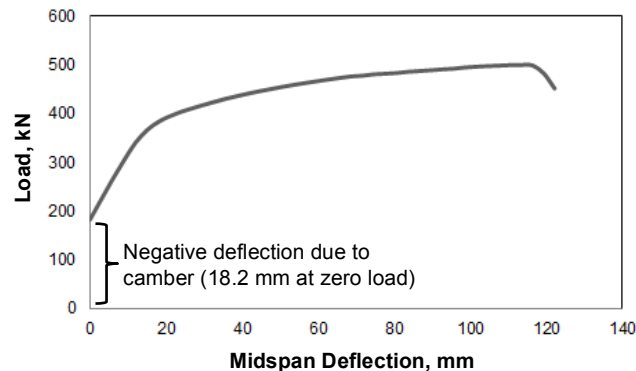


Figure 5. Load versus displacement model predictions for the 11m Long Girder under four point bending.

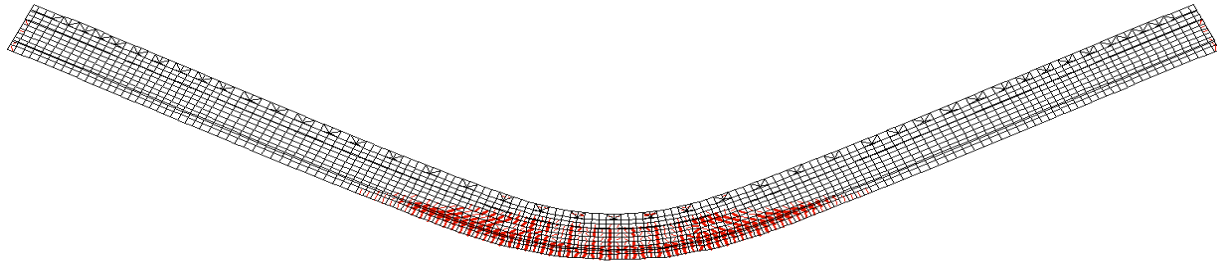


Figure 6. Failure Mode of the Modeled Girder

## 4.2 Girder Test

The first 11m long girder was delivered and set up in the I.F. Morrison Structural Lab at the University of Alberta; however, due to the schedule of the lab, the experimental test has not been completed at the time of writing, but it is scheduled for early March 2019. This second stage of the project will give experimental data related to the effect of environmental and load-induced deterioration on the bridge girder after 27 years of service.



Figure 7. The Experimental Setup of the Girder

## 4.3 Comparison of Experimental and Modeling Results

The corrosion effect of this bridge girder will be analyzed using the comparison between the experimental and modelling results. The finite element model provides a good understanding of how this 11 m long girder under initial condition will perform under testing. The experimental tests will show how the girder loses capacity, ductility, and possibly changes failure mode after deterioration. The future experimental results will show a decrease of strength of the girder from the deterioration caused by deterioration. The comparison of the experimental, modelling, and material analysis results (i.e. chloride tests on concrete, compression tests on cored cylinders, tension tests on steel, steel area loss assessments) will give a clear concept of how deterioration affected the girder.

#### 4.4 Conclusion and Recommendations

Finite element modelling of the 11 m long deteriorated girder was conducted to provide the base capacity of the damaged girder. This girder will be tested under 4 points bending test in the University of Alberta in March 2019 to investigate the corrosion effects on the girder. Based on this study, the following was observed:

1. The girder with original properties fails in flexure; concrete crushes after steel yields.
2. Test setup will give experimental results that factors in the corrosion and deterioration of the girder. The comparison between the modelling data and experimental result will give a clearer idea of how real-world timescale and deterioration mechanisms affected the capacity of this girder.

The authors recommend investigating the material properties of the girder further after testing. Because of the uncertainty of the material properties, extracting concrete and steel reinforcement (prestressed and non-prestressed) from the failed girder will give a better understanding of the actual strength of the girder. The spacing, residual cover, and condition of the bars can also be investigated by stripping of the outer layer of concrete of the failed beam. They also recommend failing the girder in shear by testing a shorter span of a future girder to give a clear idea of how this girder's shear capacity.

#### Acknowledgments

The authors wish to thank Alberta Transportation, Mike Tokar and John Alexander, as well as the Structural Engineering Technical Staff in the Morrison Structures Lab at the University of Alberta (Greg Miller and Cameron West).

#### References

- Alberta, Government Of. "Bridges and Structures." Government of Alberta Ministry of Transportation: Accessed March 01, 2019. <http://www.transportation.alberta.ca/565.htm>.
- Canadian Highway Bridge Design Code. 2014. Mississauga, Ontario: CSA Group.
- Enright, Michael P., and Dan M. Frangopol. "Service-Life Prediction of Deteriorating Concrete Bridges." *Journal of Structural Engineering* 124, no. 3 (1998): 309-17. doi:10.1061/(asce)0733-9445(1998)124:3(309).
- Mccormick, Nick, and Jerry Lord. "Digital Image Correlation." *Materials Today* 13, no. 12 (2010): 52-54. doi:10.1016/s1369-7021(10)70235-2.
- Vecchio, F.J. and Collins, M.P., (1986) "The Modified Compression Field Theory for Reinforced Concrete Elements Subject to Shear", *ACI Struct. J.*(83)2, 219-231.
- Vecchio, F. (2000). "Disturbed Stress Field Model for Reinforced Concrete: Formulation." *J. of Struct. Eng.*, ASCE, (126)9, 1070-1077.
- Wong, S. Y., and Vecchio, F. J. (2003), "Towards modeling of reinforced concrete members with externally bonded fiber-reinforced polymer composites", *ACI Struct. J.*, 100(1), 47-55.